Fermi Surface of Zirconium

S. L. ALTMANN AND C. J. BRADLEY

Department of Metallurgy, University of Oxford, Oxford, England

(Received 27 March 1964)

The Fermi surface of zirconium, as computed by means of the cellular approximation, is given. This departs fundamentally from the free-electron Fermi surface and allows an interpretation of the recent de Haas–van Alphen results obtained by Thorsen and Joseph. The right value (up to a factor of about 2) and the right angular dependence is given for four out of the five periods found by these authors. The free-electron Fermi surface, after some modification, accounted for one period only.

1. INTRODUCTION

IN the last few years a number of experimental techniques, such as the de Haas–van Alphen effect and the anomalous skin effect, have provided a very detailed knowledge of the Fermi surfaces of some metals. At the same time much progress has been achieved in the methods of computation of band structures: This has allowed an excellent agreement between theory and experiment to become apparent for those metals which Cohen[1] has called simple. These metals are those for which a pseudopotential does not depart much from a free-electron potential: Examples are the alkali and noble metals. For the transition metals, on the other hand, experiments have been more difficult and the computations, owing to uncertainty in the choice of the potential field, more unreliable. Nevertheless, we shall present in this paper a Fermi surface for zirconium metal which is the result of an *ab initio* calculation and which agrees very satisfactorily with the recent de Haas–van Alphen experiments of Thorsen and Joseph.[2] We believe that this is the first transition metal for which an agreement of this type has been reported.

2. THE METHOD OF CALCULATION

We shall refer here but briefly to the method of calculation, since it will be fully described in a forthcoming series of papers.[3] Programs have been written in this laboratory to obtain as follows the band structure of body-centered cubic, face-centered cubic, and hexagonal close-packed metals. First, by means of the cellular approximation with the method given by Altmann[4] to fit the boundary conditions, the programs provide the energy eigenvalues and eigenfunctions for any points along lines of symmetry of the Brillouin zones. For each metal the only data required in this part of the work are the crystal parameters and a potential field. For zirconium we took the experimental values $a = 3.24$ Å, $c = 5.15$ Å, and the self-consistent potential field with exchange for Zr^{4+}, kindly computed for us by Dr. D. F.

Mayers, to which the uniform charge distribution of three electrons per atom was added over the unit cell.

In a second step in the work a geometrical interpolation procedure allows the programs to compute, for any arbitrary value of $\mathbf{k}$, the energy eigenvalues for all the bands. This interpolation, which is very fast, enables us to use the Monte Carlo method in programs to determine the density-of-states curves, from which the Fermi energy of the given metal can be derived. Finally, the same interpolation scheme is used to provide contours of the Fermi surface on any required planes of the Brillouin zone. Such calculations have now been completed for Sc, Ti, V, Cr, Y, Zr, and Mo, and are in progress for Be, Ca, Al, Nb, W, and Co.

3. DESCRIPTION OF THE BRILLOUIN ZONE

In Fig. 1 we give the Brillouin zone for the hexagonal close-packed lattice, the proper orientation of which with respect to the direct lattice axes can be seen in Fig. 2.

In order to show up the sticking together of the bands on the top and bottom faces of the Brillouin zone, it is more convenient to use a double Brillouin zone as shown in Fig. 3. This is obtained from the simple zone of Fig. 1 by adding to it the parts drawn in dashed lines in Fig. 3. We also show in this figure a wedge that forms the basic domain of the Brillouin zone in the sense that the determination of any energy surface over it gives
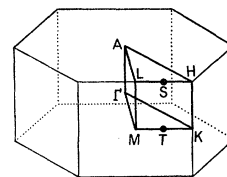

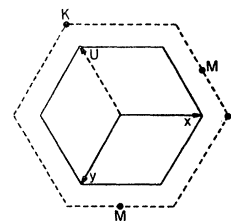FIG. 1. The Brillouin zone for the hexagonal close-packed lattice.

FIG. 2. The dashed line is the trace of the Brillouin zone in an arbitrary scale. z is perpendicular to the plane of the drawing. The axis u is not used in this paper and a dot is placed in the relevant position of the symbols for lines and planes.

[1] Lecture at the Institute of Physics and Physical Society Solid State Conference, Bristol, January 1964.
[2] A. C. Thorsen and A. S. Joseph, Phys. Rev. **131**, 2078 (1963).
[3] See S. L. Altmann and C. J. Bradley, Phys. Letters **1**, 336 (1963) for a preliminary communication.
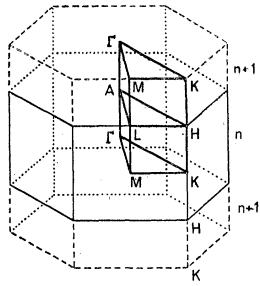[4] S. L. Altmann, Proc. Roy. Soc. (London) **A244**, 141, 153 (1958).

FIG. 3. The double zone. The n and $n+1$ bands are plotted in the domains shown.

FIG. 5. Fifth and sixth bands.

that energy surface for the whole of the double zone. It is enough to apply a reflection first on the lower horizontal face of the wedge, then on its ΓML face, and finally to apply sixfold symmetry about the axis ΓA. It should also be remembered that in order to study the electron orbits, it is convenient to use the periodically extended scheme in which the hexagonal prism of Fig. 3 is repeated to fill all space. (This amounts to applying reflection symmetry with respect to the faces of the zone.)

The basic dimensions of the Brillouin zone for zirconium are $\Gamma A = 0.610$ Å^{-1}, $\Gamma K = 1.298$ Å^{-1}, $\Gamma M = 1.122$ Å^{-1}, and $MK = 0.649$ Å^{-1}.

4. THE CALCULATED FERMI SURFACE FOR ZIRCONIUM

Our results show that bands 1 and 2 are full in zirconium. The contours of the Fermi surface for bands 3 and 4 are shown in Fig. 4. The left-hand side of the figure gives the contours on the external surface of the basic domain shown in Fig. 3; it can be seen that by appropriately folding this picture this domain is obtained. The right-hand side of the figure gives the section of the Fermi surface on a vertical plane of the domain through the ΓA axis and which bisects MK. Results for the bands 5 and 6 are displayed in the same manner in Fig. 5. In these figures the regions shaded are those occupied by electrons. From these contours the Fermi surfaces are easily drawn and they are displayed in Figs. 6 and 7 (see also Fig. 10).

The most notable features of the Fermi surface are the spheroidal pockets of holes around L in the 3rd and
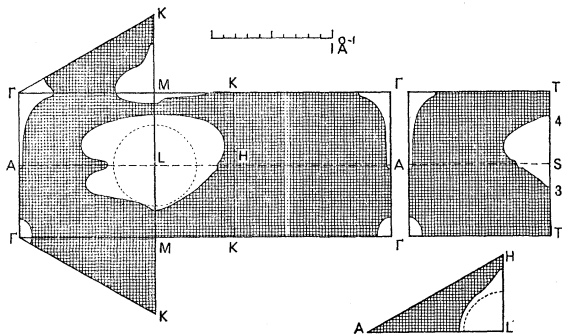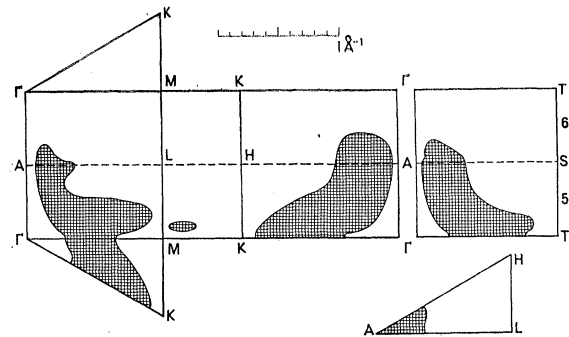
4th bands, with deep grooves along their equatorial planes, and the torus-like monster with twenty four necks in the 5th and 6th bands.

We should like to stress first that the proposed Fermi surface bears no resemblance to the free-electron one (see Thorsen and Joseph[2]), secondly that the results given here are exactly as obtained from the computer without any modifications, and thirdly that they were obtained before the experimental results of Thorsen and Joseph were available to us.

5. THE DE HAAS–VAN ALPHEN RESULTS OF THORSEN AND JOSEPH

In this and the following sections all periods will be measured in period units of 10^{-8} G^{-1}, to be abbreviated pu, and all the lengths and areas in the reciprocal space in Å^{-1} and Å^{-2}, respectively. In these units the relation between the period and the extremal area A of the Fermi surface is $P = 0.9546/A$.

Thorsen and Joseph measured the variation of the de Haas–van Alphen periods when the magnetic field is rotated in three planes: $(1\bar{1}.0)$, (10.0), and (00.1). These are identified in Fig. 2 with the following planes, respectively, in the Brillouin zone: (i) a vertical plane through ΓA and ΓK, (ii) a vertical plane through ΓA and ΓM, (iii) a horizontal plane. In this manner, Thorsen and Joseph obtained the following results. There is a period α that has a fairly constant value near
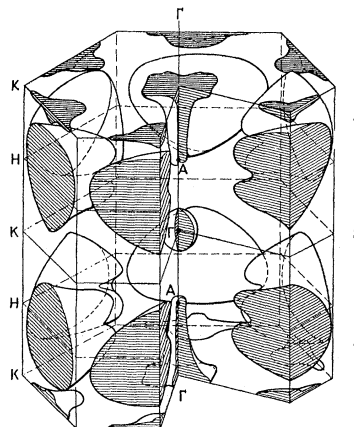

FIG. 4. Third and fourth bands.

FIG. 6. The Fermi surface for the third and fourth bands. The volumes enclosed by the surfaces drawn contain holes.

3 pu in all directions. When the magnetic field is along the directions [00.1], [10.0], and [1Ī.0] (i.e., ΓA, ΓK, and ΓM, respectively) the periods are 2.85, 2.67, and 2.65 pu, respectively. The period α is dominant in all directions except [00.1] where a period β is dominant. This period is a little smaller than α, varies from 2.6 to 2.3 pu and disappears when the magnetic field is tilted some 25° away from the [00.1] direction. There is a third period γ of about 2 pu, which also appears along [00.1] and disappears when the field is tilted some 30° away from [00.1]. A fourth period δ, about 3.5 pu, can be seen only along or very near the [10.0] (ΓK) direction. It disappears when the field is tilted some 10° upwards from the horizontal (00.1) plane or is moved by the same amount in this latter plane from [10.0] towards [1Ī.0] (i.e., from ΓK towards ΓM). Finally, there is a period ε just over 2.5 pu that appears when the field is in the (1Ī.0) plane at an angle between 30° and 45° to the [00.1] direction.

We shall see in the following sections that we can account for all the above periods except ε. We cannot expect a very accurate numerical fit, owing to the complexity of the metal. Factors of up to 2 in the periods will sometimes appear, which mean that we get the average radius of such orbits wrong by about 40%. This is not too bad an agreement for such complex

Fig. 7. The Fermi surface for the fifth and sixth bands. The volume enclosed by the surface drawn contains electrons.
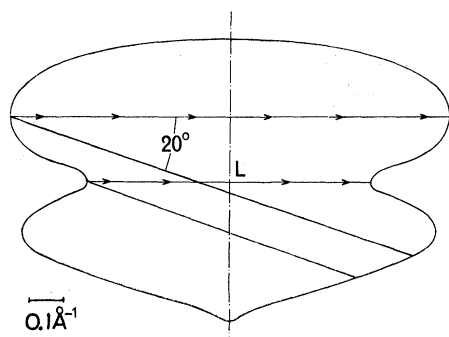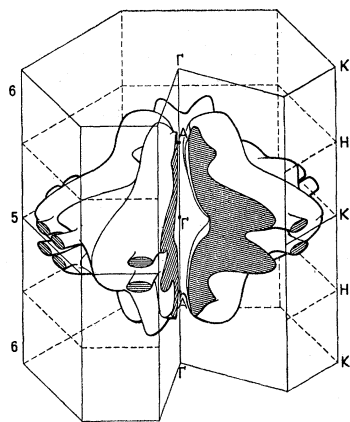

Fig. 8. Angular variations of β. The curve given is the section of the third and fourth band Fermi surface in the plane ΓML. The vertical axis of the figure coincides with the line ML.
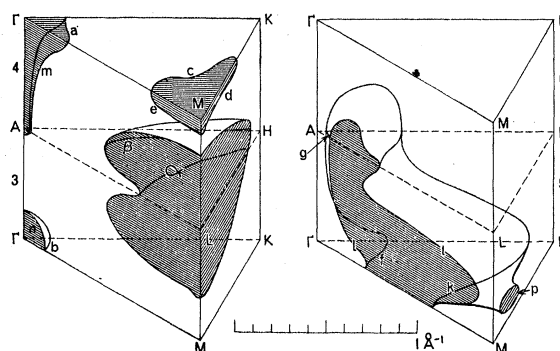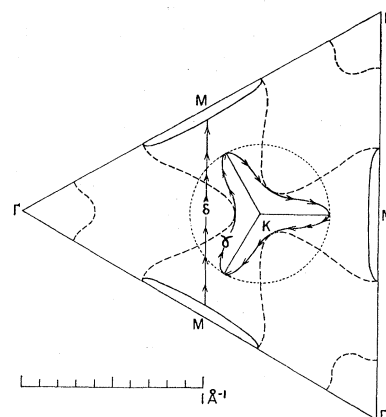

Fig. 9. The γ and δ periods.

Fig. 10. Some orbits given in the basic domain of Fig. 3. The volumes enclosed by the surfaces drawn contain holes for the third and fourth bands and electrons for the fifth and sixth bands.

shapes as we have, but we consider it more important that we account correctly for the angular dependence of these periods, since this is intimately related to the topology of the Fermi surface. It should be noticed, as a comparison, that Thorsen and Joseph had to distort substantially the free-electron Fermi surface and even then they could not account for any period other than α.

6. THE α AND β PERIODS

It is clear that the fairly constant α period must be identified with the spheroidal pocket of holes around L in the 3rd and 4th bands. The sections of Fig. 4 give the following periods (experimental values in brackets):

Direction	Period (pu)
[00.1]	1.9(2.85)
[10.0]	1.3(2.67)
[1Ī.0]	1.4(2.65).

The agreement is just fair but the adequacy of the fit is perhaps better gauged by comparing the calculated sections with the circles whose areas give the experimental periods: These are given in broken lines in Fig. 4.

The spheroidal pocket around L has another extremal section perpendicular to the [00.1] direction, as can be seen in Figs. 6 and 10, which we identify with the β

period. In fact, it agrees with the following experimental facts: (i) Since the Fermi surface has smaller curvature for this orbit than at the equator, β is the dominant period along [00.1]. (ii) β is correctly smaller than α; its calculated value is 1.1 pu (experimental 2.6). (iii) It disappears at about 20° from [00.1]. This is shown in Fig. 8, where it can be seen that when the field exceeds this angle the spheroidal body ceases to have two extremal sections perpendicular to the same direction.

7. THE γ AND δ PERIODS

The γ and δ orbits are identified in Fig. 9, which is drawn in the periodically extended scheme. The empty segments of the KM lines correspond to the regions where the necks in two different cells join each other. The contour of the necks forms a three-cornered rosette, the inside of which is occupied by holes. We identify this orbit, which embraces a very flat region of the Fermi surface, with the γ period. The computed period is 5.15 pu (experimental 2.6, compare also the circle drawn in broken lines in Fig. 9 that gives the experimental section). On account of the flatness of the Fermi surface in this region this period should disappear when the field is tilted away from [00.1], which agrees with experiment.

We identify the δ period with an orbit perpendicular to ΓK and that embraces two necks. This orbit has the shape of a very flat ellipsoidal curve perpendicular to the plane of Fig. 9 and whose major axis is the line shown in it. The estimated section gives a period of 3.8 pu (experimental 3.4). What is more important, it follows from the shape of the orbit that the period should disappear when we move the field in Fig. 9 a little upwards from the ΓK direction. Also, when the field goes from ΓK to ΓM, this orbit is replaced by another one around a single neck which corresponds to

TABLE I. Periods of the orbits given in Fig. 10.

Direction	Orbit	Period (pu)
[00.1]	a	4.7
	b	30
	c	3.3
	g	40
	f	2.3
	k	0.4
[10.0]	e	11
	m	4.1
	n	20
	l	1.4
[1$\bar{1}$.0]	d	17
	p	56

a very large period outside the range observed by Thorsen and Joseph. This angular dependence is exactly that described in Sec. 5.

8. OTHER PERIODS

In Fig. 10 we identify with lower case roman letters parts of a number of other possible orbits, the corresponding periods of which are given in Table I. We shall comment briefly on those periods in a range of the order observed by Thorsen and Joseph. Period a would decrease and c would increase rapidly with the angle from [00.1], so much so that after a few degrees it would take a very large value. Period f would behave similarly to β and γ but would not have a sharp cutoff. No indication was found by Thorsen and Joseph of the orbits m and l perpendicular to [10.0].

9. SPIN ORBIT SPLITTING

As shown by Cohen and Falicov[5] spin orbit interaction removes the sticking together of the bands on the ALH face except along the AL line. The double zone scheme that we have used is not then strictly correct. However, the maximal splittings occur at H, where, as can be seen from Fig. 10, they would not affect much our orbits. Also since the expected splittings are small, of the order of 10^{-2} eV, magnetic breakthrough can be expected,[6] which would restore the double-zone orbits. We have not considered it worthwhile, therefore, to introduce spin-orbit coupling effects at this stage, although the study of such effects will be necessary if more detailed experimental evidence becomes available.

[5] L. M. Falicov and M. H. Cohen, Phys. Rev. 130, 92 (1963).
[6] M. H. Cohen and L. M. Falicov, Phys. Rev. Letters 7, 231 (1961).